TPEPICO Spectroscopy of Vinyl Chloride and Vinyl Iodide: Neutral and Ionic Heats of Formation and Bond Energies

Nicholas S. Shuman, Melony A. Ochieng, Bálint Sztáray,[†] and Tomas Baer*

Department of Chemistry, University of North Carolina, Chapel Hill, North Carolina 27599-3290

Received: January 24, 2008; Revised Manuscript Received: March 25, 2008

The 0 K dissociative ionization onsets of $C_2H_3X \rightarrow C_2H_3^+ + X$ (X = Cl, I) are measured by threshold photoelectron-photoion coincidence spectroscopy. The heats of formation of C_2H_3Cl ($\Delta H^0_{f,0K} = 30.2 \pm 3.2$ kJ mol^{-1} and $\Delta H^0_{f,298K} = 22.6 \pm 3.2$ kJ mol^{-1}) and C_2H_3I ($\Delta H^0_{f,0K} = 140.2 \pm 3.2$ kJ mol^{-1} and $\Delta H^0_{f,298K} = 131.2 \pm 3.2$ kJ mol^{-1}) and C−X bond dissociation enthalpies as well as those of their ions are determined. The data help resolve a longstanding discrepancy among experimental values of the vinyl chloride heat of formation, which now agrees with the latest theoretical determination. The reported vinyl iodide heat of formation is the first reliable experimental determination. Additionally, the adiabatic ionization energy of C_2H_3I (9.32 ± 0.01 eV) is measured by threshold photoelectron spectroscopy.

Introduction

Reported values of the thermochemistry of the vinyl monohalides show surprisingly high levels of uncertainty considering the simplicity of the monohalide structures, their importance in atmospheric and industrial chemistry, and their common research use as organic reagents and as photolytic precursors to the vinyl radical.

The vinyl fluoride heat of formation has only one experimental determination, by rotating bomb calorimetry in 1970.[1] Similarly, the heat of formation of vinyl bromide had long been dependent on a single measurement[2] dating to the 1950s, a value that has since been corrected by 5 kJ mol^{-1} as a result of our recent threshold photoelectron photoion coincidence (TPEPICO) study.[3]

Although the heat of formation of vinyl chloride has received much more attention, reported experimental measurements vary widely. The 298 K values (kJ mol^{-1}) include 21.0 and 22.7[4] determined by hydrochlorination equilibrium measurements over two temperature ranges, 22.7[5] derived from the measured enthalpy of polymerization, 27.5[6] as a lower limit determined by photoionization, 35.2[7] based on hydrochlorination calorimetric measurements, and 38.1[8] based on hydrogenation calorimetry. Manion[9] published a recent critical review of these experimental measurements and compared them to an ab initio calculated heat of formation by Colegrove and Thompson[10] as well as group-additivity estimates of Luo and Holmes[11] and Aflassi et al.[12] Manion recommended a 298 K heat of formation of 22.0 ± 3 kJ mol^{-1}, which agrees quite well with a very recent high-level ab initio calculated value of 22.2 ± 2 kJ mol^{-1}.[13,14] Despite this apparent consensus, the fact remains that no recent, reliable experimental determination exists. Compounding the problem, two major and frequently quoted compilations of thermochemical data, *The Heats of Formation of Organic Compounds* by Pedley[15] and *Bond Energies of Organic Compounds* by Luo,[16] recommend the suspiciously high values of Lacher and Sheng, respectively. A third compilation, T*hermodynamic Properties of Individual Subtances* by Gurvich, Veyts, and Alcock[17] recommends a value of 23.0 ± 2.1 kJ mol^{-1}, in line with the most recent calculated values.

Vinyl iodide has received little attention either experimentally or theoretically, and no reliable value for its heat of formation exists. A lone experimental determination of the C−I bond dissociation enthalpy (BDE), derived from the maximum energy release in the photodissociation of vinyl iodide,[18] implies a vinyl iodide 298 K heat of formation of 143.2 kJ mol^{-1}, 5 kJ mol^{-1} less positive than a value calculated by G2(ECP) theory,[19] whereas group-additivity estimated[11] values suggest a heat that is 20 kJ mol^{-1} less positive.

In this study, we use TPEPICO spectroscopy to study the dissociative ionization of vinyl chloride and vinyl iodide. We accurately measure the threshold energy for production of vinyl ion from the ground state of the reactant, the so-called 0 K dissociation onset (E_o) of

$$C_2H_3X \xrightarrow{h\nu} C_2H_3X^+ \rightarrow C_2H_3^+ + X \qquad (X = \mathrm{Cl, I}) \qquad (1)$$

By combining these data with previously determined thermochemical data of the vinyl radical and ion,[3] we can establish the enthalpies of formation and C−X BDEs of both the neutrals and cations within the uncertainty of the vinyl ion heat of formation, 3 kJ mol^{-1}. The methodology is shown schematically in Figure 1. Along with our recent vinyl bromide determination by using the same methodology, we can report new experimental values for all three vinyl monohalides that are anchored to the same vinyl ion heat of formation and are thus internally consistent within the uncertainty of the measured dissociation onsets of about 1 kJ mol^{-1}.

Experimental Methods

The TPEPICO spectroscopy apparatus has been described in detail elsewhere.[20] Briefly, sample vapor is introduced to a high-vacuum chamber and ionized by vacuum-ultraviolet radiation from a hydrogen discharge lamp dispersed by a 1 m normal-incidence monochromator. The resulting ions and electrons are accelerated in opposite directions by a 20 V cm^{-1} (40 V cm^{-1} for vinyl chloride) voltage gradient. Velocity focusing optics direct all electrons with zero velocity transverse to the acceleration axis onto a Channeltron (Burle) detector centered on the

---

* E-mail: baer@unc.edu.

[†] Current address: Chemistry Department, University of the Pacific, Stockton, CA 95211-0110

10.1021/jp8007255 CCC: $40.75

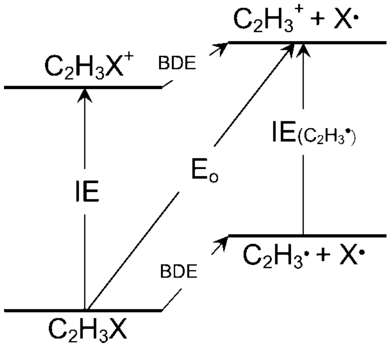

Figure 1. Thermochemical scheme for deriving the C_2H_3X heat of formation. Arrows indicate the 0 K dissociation onset (E_o, see text), relevant ionization energies (IE), and derived C−X BDEs.

acceleration axis. A second Channeltron detector centered off-axis collects a fraction of the translationally excited (hot) electrons. A mask with a 1.4 mm diameter center hole and a 3 × 5 mm rectangular off-axis opening defines the electron trajectories that are collected. The off-axis signal collected simultaneously with the on-axis signal allows for subtraction of the hot-electron background present in the threshold electron collection.

Ions are collected in either of two experimental set-ups. In the linear TOF mass spectrometer (LinTOF), ions are accelerated in two stages to −260 V (vinyl iodide) or −520 V (vinyl chloride) before entering a 26 cm drift region and impact a tandem 25 mm microchannel plate (MCP, Burle) in a chevron configuration. In the reflecting TOF mass spectrometer (ReTOF), the ions are accelerated to 100 V in the 5 cm long acceleration region, drift for 30 cm at 100 V to the single stage reflectron, and are reflected into the final 30 cm long drift tube to the MCPs. The ReTOF allows for higher mass resolution than the LinTOF.

Ion TOFs are determined by the time difference between the electron (start signal) and the ion (stop signal) detection. Two spectra, one for the on-axis electrons and one for the off-axis electrons, are collected simultaneously. The use of time-to-pulse height converters in TOF-spectra collection necessitates a single-start/single-stop method, wherein the first ion signal after an electron start effectively stops the acquisition cycle regardless of whether that ion originated in the same ionization event as the electron. Ions detected while no start signal is active as well as electrons detected while a start signal is active (on either detector) are ignored.

The same instrument is used to measure threshold photoelectron spectra. Electron counts are collected on both the ring and center Channeltrons, and photon flux is monitored by a photomultiplier tube while the monochromator is scanned at a rate of 0.5 Å min^{-1}.

Results

Representative ion TOF mass spectra of the photoioinzation of C_2H_3Cl at photon energies between 12.3 and 13.9 eV obtained with the LinTOF arrangement at a sample temperature of 258 K are shown in Figure 2. Spectra were corrected for paralysis effects as discussed in the Appendix, and the relative peak areas of the parent and all fragment ions were corrected for mass-dependent detection efficiency of the MCPs and for hot-electron contamination. To correct for hot-electron contamination, spectra of coincidences involving the off-axis Channeltron (due exclusively to hot electrons) were scaled by an empirically determined factor and subtracted from the simultaneously obtained on-axis spectra. The resulting spectra reflect only ionization events which produced threshold (zero kinetic energy) electrons. This procedure has been described and tested in previous publications.[20,21]

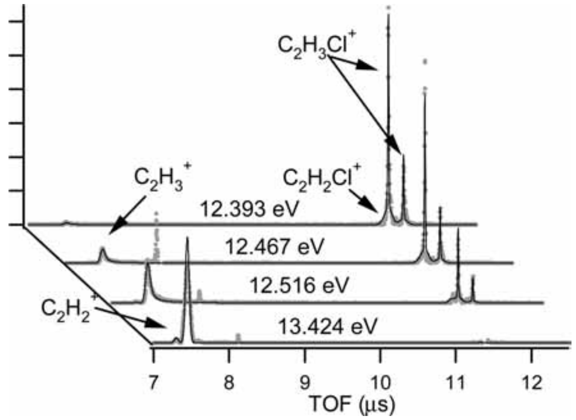

Figure 2. TOF spectra of C_2H_3Cl photoionized at various indicated photon energies. Gray dots are experimental points, and black lines are best-fit curves as described in the text. The peak at 8.1 μs is due to oxygen present in the sample line.

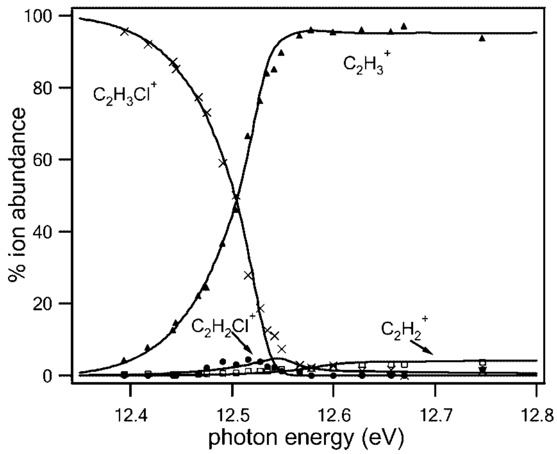

Figure 3. Breakdown diagram of C_2H_3Cl at photon energies between 12.35 and 12.8 eV. Symbols are experimental percent abundances for $C_2H_3Cl^+$, $C_2H_3^+$, $C_2H_2^+$, and $C_2H_2Cl^+$. Lines are best-fit curves as described in the text.

Over the photon energies investigated, dissociation of $C_2H_3Cl^+$ proceeds through several competing pathways:

$$C_2H_3Cl^+ \rightarrow C_2H_3^+ + Cl \tag{a}$$

$$C_2H_3Cl^+ \rightarrow C_2H_2^+ + HCl \tag{b}$$

$$C_2H_3Cl^+ \rightarrow C_2H_2Cl^+ + H \tag{c}$$

$$C_2H_3Cl^+ \rightarrow C_2HCl^+ + H_2 \tag{d}$$

The breakdown diagram, which shows relative product ion abundances as a function of photon (and therefore ion internal) energy, of vinyl chloride is shown in Figure 3. The vinyl ion product, channel (a), dominates the reaction at all energies, despite the acetylene ion product, channel (b), being slightly (5 kJ mol^{-1}) energetically favored. An H-loss product, channel (c), is also observed with an onset similar to that of (a) and (b). A very small amount of product is produced through the H_2-loss channel, (d), at energies above 13 eV (not shown in Figure 3).

We have similarly obtained ion TOF mass spectra of the photoionization of room temperature (298 K) C_2H_3I at photon energies between 11.0 and 11.5 eV with both the LinTOF and the ReTOF arrangements. These spectra have been corrected

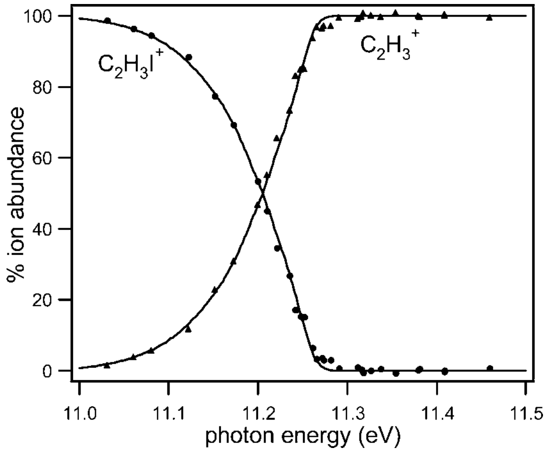

Figure 4. Breakdown diagram of C_2H_3I photoionized at energies between 11.0 and 11.5 eV. Circles ($C_2H_3I^+$) and triangles ($C_2H_3^+$) are experimental points. Lines are best-fit modeled breakdown curves as described in the text.

in the same manner as the vinyl chloride spectra. Spectra show the presence of just two peaks, corresponding to the parent ion, $C_2H_3I^+$, and a single fragment ion, $C_2H_3^+$; this dissociation is analogous to product channel (a) of the vinyl chloride dissociation. Unlike the vinyl chloride, no other dissociation channels were observed at photon energies below 14.4 eV, the maximum energy output of our light source. Symmetric fragment ion peak shapes observed in all spectra indicate that the dissociation of $C_2H_3I^+$ at these energies occurs on a time scale more rapid than that measurable with our instrument, setting a lower bound on the rate constant of the dissociation of about 10^7 s^{-1}. The breakdown diagram for C_2H_3I appears in Figure 4.

The adiabatic IE of vinyl chloride has recently been measured by zero electron kinetic energy photoelectron spectroscopy to be 10.0062(3) eV,[22] in excellent agreement with other recent measurements.[23–25] In contrast, the IE of vinyl iodide has been less well established, with various photoelectron spectroscopy measurements reporting values between 9.25 and 9.32 eV[26–29] and with unreported uncertainties in all cases. We have recorded the threshold photoelectron spectrum of vinyl iodide at 253 K (Figure 5) and determined the adiabatic IE of vinyl iodide to be 9.32 ± 0.01 eV.

Extraction of Thermochemistry and Bond Energies

Our group has previously described in detail the modeling of parallel ion dissociations by using the statistical theory of unimolecular decay.[21] Briefly, for a single fast dissociation (one in which all ions with sufficient energy to dissociate do so in less than 0.1 μs), such as in the case of vinyl iodide here, one need to consider only the thermal energy distribution of the dissociating ion and can model the breakdown diagram by

$$A_p(h\nu) = \int_0^{E_o - h\nu} P(E)\,dE \qquad (2)$$

$$A_f(h\nu) = \int_{E_o - h\nu}^{\infty} P(E)\,dE \qquad (3)$$

where A_p and A_f are the parent and fragment ion abundances respectively, E_o is the 0 K dissociation onset, E is the internal energy of the parent ion, and $P(E)$ is the parent ion thermal energy distribution defined by

$$P(E) = \rho(E)\,e^{(-E/kT)} \qquad (4)$$

where $\rho(E)$ is the density of states of the neutral parent molecule. This approach assumes that the energy distribution of the neutral molecule is faithfully transposed to the parent ion.

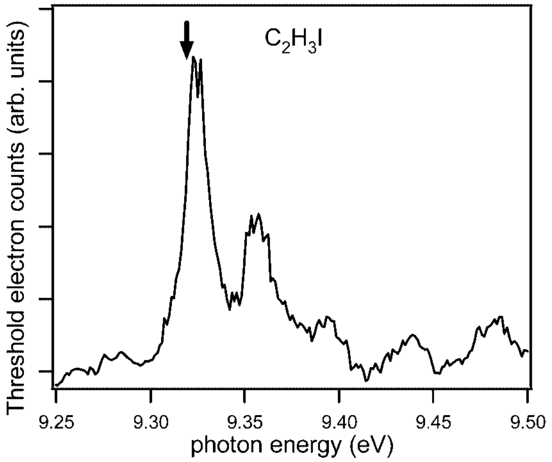

Figure 5. Threshold photoelectron spectrum of C_2H_3I from 9.25 to 9.50 eV. The arrow indicates the determined adiabatic IE.

TABLE 1: TPEPICO Vinyl Chloride and Vinyl Iodide 0 K Ionization and Dissociation Onsets

neutral	IE (eV)	product channel	E_o (eV)
C_2H_3Cl	10.0062[a]	$C_2H_3^+$ + Cl	12.530 ± 0.010
C_2H_3I	9.32 ± 0.01	$C_2H_3^+$ + I	11.262 ± 0.010

[a] From refs 22 and 25.

When competing parallel reactions are present, such as in the case of vinyl chloride, the relative rates of each channel must be considered. We observe three channels, (a), (b), and (c), with similar onsets, and because each is a fast dissociation, we have no experimental information about their absolute rates. Five parameters determine the relative kinetics of the reactions: the activation barriers of each of the three channels and the difference in activation entropies between (a) and (b) and between (a) and (c) (with the difference between (b) and (c) then determined). A modeling program is used to calculate the breakdown curve for a given set of values of these parameters and perform a multidimensional optimization in order to minimize an error function with respect to the experimentally determined breakdown diagram. The optimized parameters produce calculated TOF spectra in excellent agreement with experiment at all energies (Figures 2 and 3). The best-fit onset of channel (a), the vinyl ion channel, is robustly determined by the fitting within 0.010 eV. The very small yields for the minor dissociation channels prevent any reasonable determination of their onsets; however, it is important to note that the calculated onset of channel (a) remained largely the same for any reasonable parameters used to describe the other channels. Results for X loss from C_2H_3X are summarized in Table 1.

The 0 K heat of formation of C_2H_3X is determined by

$$\Delta H^o_{f,0K}(C_2H_3X) = \Delta H^o_{f,0K}(C_2H_3X^+) + \Delta H^o_{f,0K}(X) - E_o \qquad (5)$$

where E_o is the measured 0 K dissociation onset of the vinyl ion product channel. Because the measured onset energy is good within ±1 kJ mol^{-1}, the error in the derived heat of formation is limited by the accuracy to which the 0 K heats of formation of $C_2H_3^+$ and X (X=Cl, I) are determined. $\Delta H^0_{f,0K}$ value of Cl and I are well-known, whereas the $\Delta H^0_{f,0K}$ value of $C_2H_3^+$ is less well established (see Table 2).

The 298 K heat of formation of C_2H_3X can be determined from the 0 K value by the standard thermochemical cycle:

$$\Delta H^0_{f,298K}(C_2H_3X) = \Delta H^0_{f,0K}(C_2H_3X) + [H^0_{298K} - H^0_{0K}](C_2H_3X) - [H^0_{298K} - H^0_{0K}](C,H,X) \quad (6)$$

We calculate $[H^0_{298K} - H^0_{0K}](C_2H_3Cl)$ to be 11.8 kJ mol^{-1} and $[H^0_{298K} - H^0_{0K}](C_2H_3I)$ to be 12.4 kJ mol^{-1} by using the harmonic vinyl halide vibrational frequencies calculated at the B3LYP/6-311G** level and use literature values of the thermal enthalpy corrections for the reference states.[30]

Additionally, the BDEs of the C−X bond in C_2H_3X are determined by

$$\mathrm{BDE} = \Delta H^0_{f,298K}(C_2H_3) + \Delta H^0_{f,298K}(X) - \Delta H^0_{f,298K}(C_2H_3X) \quad (7)$$

The C−X BDEs of the vinyl halide ions are determined by the difference of the measured vinyl ion 0 K dissociation onset and the adiabatic IE of the vinyl halide. The adiabatic IE also determines the 0 K heat of formation of the vinyl halide ions relative to the 0 K heats of formation of the neutrals. All thermodynamic data are summarized in Table 3.

TABLE 2: Ancillary Heats of Formation

	$\Delta H^0_{f,0K}$ (kJ mol^{-1})	$\Delta H^0_{f,298K}$ (kJ mol^{-1})	$H_{298} - H_0$
C_2H_3[a]	298.9 ± 1.7	295.4 ± 1.7	11.3
$C_2H_3^{+}$[a]	1119.6 ± 3.0	1116.1 ± 3.0	11.3
Cl[b]	119.621 ± 0.006	121.301 ± 0.008	6.272
I[b]	107.16 ± 0.04	106.76 ± 0.04	6.197

[a] From ref 3. [b] From ref 30.

TABLE 3: Summary of TPEPICO Determined ΔH^o_f and Bond Energies (kJ mol^{-1}) of Vinyl Halides

	ΔH^o_f		C−X BDE		
	0 K	298 K[a]	0 K	298 K[a]	$H_{298} - H_0$
C_2H_3Cl	30.2 ± 3.2	22.6	388.3 ± 3.1	394.1	11.8
$C_2H_3Cl^+$	995.7 ± 3.2	988.4	243.6 ± 1.0	249.0	12.1
C_2H_3Br[b]	89.1 ± 3.2	74.1	327.7 ± 3.2	333.2	12.1
$C_2H_3Br^{+}$[b]	1036.6 ± 3.2	1021.9	200.9 ± 1.0	206.3	12.4
C_2H_3I	140.2 ± 3.2	131.2	265.9 ± 3.1	271.0	12.4
$C_2H_3I^+$	1039 ± 3	1031	187.3 ± 1.4	196.2	12.6

[a] Uncertainties in 298 K values are identical to those in 0 K values. [b] From ref 3.

TABLE 4: Calculated Enthalpy of Reaction of $CH_3I + C_2H_4 \rightarrow CH_4 + C_2H_3I$ and Derived Enthalpy of Formation of C_2H_3I at Varying Levels of Theory

method[a]	$\Delta H^0_{r,0K}$ (kJ mol^{-1})	$\Delta H^0_{f,0K}(C_2H_3)I$ (kJ mol^{-1})
B3LYP/6-311G**	−11.1	140.5
CCSD/6-311G**	−10.5	141.1
B3LYP/aug-cc-PVTZ[b]	−10.9	140.9
CCSD(T)/aug-cc-PVTZ[b,c]	−12.6	139.2

[a] All basis sets from ref 34. [b] SDB-aug-cc-PVTZ pseudopotential basis set used for I. [c] Geometries optimized and zero-point energies calculated at the B3LYP/aug-cc-PVTZ level.

Discussion

Previous experimental determinations of the heat of formation of vinyl chloride have varied widely, as described in detail by Manion.[9] Values from heat of equilibrium experiments performed by Levanova et al.,[4] derivation of the heat of formation of vinyl chloride from its heat of polymerization,[5] and group-additivity methods[12,31] are clustered around 22 kJ mol^{-1} at 298 K. Two calorimetric values reported by Lacher et al.[7,8] are in good agreement with one another (38.1 and 35.2 kJ mol^{-1}) but are such outliers to other determinations that they suggest that the experiments may have suffered from a systematic error. A third outlying value (27.5 kJ mol^{-1}) derived from the appearance energy of vinyl ion in a photoionization experiment by Sheng et al.[6] is also suspect because the appearance energy reported in the text differs from that indicated in the published figure by over 10 kJ mol^{-1}. Based on a review of these experimental and other calculated values, Manion excludes the outlying values of Lacher et al. and suggests a value for the 298 K heat of formation of 22.0 ± 3 kJ mol^{-1}. Our own experimental TPEPICO value of 22.6 ± 3.2 kJ mol^{-1} agrees extremely well with the value recommended by Manion. Finally, the very recent high-level ab initio calculated value of 22.2 ± 2 kJ mol^{-1} [13] is in accord with these conclusions, as is a G2 calculated value of 21.8 kJ mol^{-1}.[19] The strong agreement among these results suggests that the uncertainty in the heat of formation of vinyl chloride is in fact now less than the 2−3 kJ mol^{-1} reported for each individual determination.

The 298 K C−I BDE of C_2H_3I has previously been determined by Cao et al. by measuring the maximum kinetic energy release in the photodissociation of C_2H_3I at 248 nm.[18] The resulting value of 259 ± 4 kJ mol^{-1} is 12 kJ mol^{-1} lower than that reported here, and the two measurements are outside of the mutual uncertainties. However, Cao's analysis assumes an accuracy of ∼2 kJ mol^{-1} in their energy determination and zero uncertainty in the modeled fit to the kinetic-energy release curve. Inspection of their published data suggests that this has likely resulted in an underestimation of the uncertainty in the BDE measurement. It seems likely that Cao's measurement and ours, in fact, agree fairly well, with our reported value improving the accuracy of the BDE and significantly lowering the uncertainty.

Our measured heat of formation of C_2H_3I is significantly (∼17 kJ mol^{-1}) lower than that previously calculated by using the G2(ECP) theory.[19] It is interesting that these same calculations rather accurately reproduce the experimental values of the heats of formation for vinyl fluoride, chloride, and bromide (within 7, 1, and 5 kJ mol^{-1}, respectively). However, these heats were calculated by ab initio heats of atomization, which in general are more susceptible to systematic inaccuracies in the method than are heats of formation derived from the calculated heat of an isodesmic reaction (where those inaccuracies tend to cancel out).

To compare to the G2 calculation and examine the reliability of our experimental result, we calculated the enthalpy of reaction of the isodesmic reaction

$$CH_3I + C_2H_4 \rightarrow CH_4 + C_2H_3I \quad (8)$$

by DFT and ab initio methods with a variety of basis sets using the Gaussian 03 program suite.[32] An analogous approach has been used to accurately calculate the heat of formation of vinyl bromide[3] and to calculate a heat of formation of vinyl chloride[10] in excellent agreement with the experimental value presented here. By using a literature 0 K enthalpy of formation of CH_4(−66.63 ± 0.3)[33] and converting the well established 298 K values[15] of CH_3I and C_2H_4 to 0 K (24.0 ± 0.8 and 60.4 ± 0.3, respectively), we can determine the 0 K enthalpy of formation of C_2H_3I. Calculated values are presented in Table 4 and are in excellent agreement with the experimental values reported here. The average calculated value, 140.5 kJ mol^{-1}, is well within the uncertainty of our measured value of 140.2 ± 3.2 kJ mol^{-1}.

The TPEPICO determined heats of formation and C−X BDEs of the vinyl halide neutrals and ions in Table 3 show uncertain-

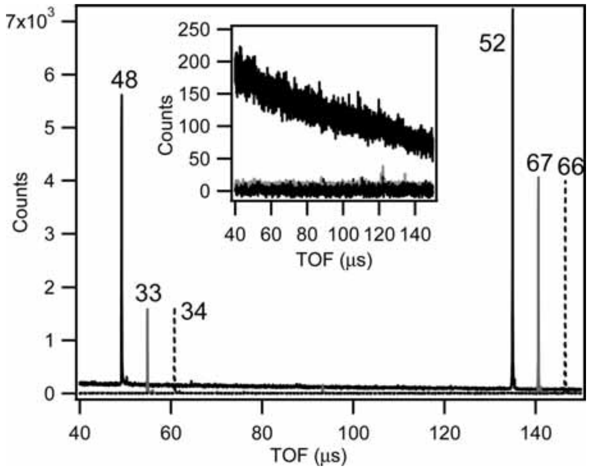

Figure A1. TOF spectra of C_2H_3I photoionized at 11.20 eV at high (8000 c/s, black) and low (1000 c/s, gray) conditions and the paralysis-corrected high count spectrum (dashed). The gray and dashed traces are offset horizontally for clarity (TOFs are identical to those in the black trace); spectra are not offset vertically. Percent ion abundances for daughter and parent ions appear above each peak. The inset shows just the false coincidence background spectra for the high and low ion count spectra in which the true coincidence peaks have been removed for clarity.

ties of ~3 kJ mol^{-1}. Because the error in the onset measurements are about 10 meV (1 kJ mol^{-1}), this uncertainty primarily reflects the uncertainty in the heat of formation of the vinyl ion (Table 2). Because the derived values for the vinyl chloride, bromide, and iodide and their ions are all anchored by the same species (the vinyl ion), all values reported here are internally consistent within the uncertainty in the measured appearance energies, about 1 kJ mol^{-1}. If any one of these heats is independently determined to an uncertainty less than that of the vinyl ion, the uncertainties in all of the other derived values (including the heat of the vinyl ion) will be reduced accordingly. Evaluation of the strong agreement between our reported value for the vinyl chloride heat of formation and the independent evaluated result of Manion and calculation by Harding et al. suggests a 298 K value of about 22.2 ± 1.5 kJ mol^{-1} along with appropriate adjustments to the values and uncertainties reported here in Tables 2 and 3. However, such a complete evaluation is beyond the scope of this paper and best left to projects such as the Active Thermochemical Tables of Ruscic et al.[35]

Appendix

Paralysis Correction. Because of the high count rate and the long flight time difference between the $C_2H_3I^+$ parent ion and the much lighter $C_2H_3^+$ vinyl ion, the dissociation of vinyl iodide also provides a testing ground to evaluate a systematic error in single-start/single-stop coincidence measurements caused by paralysis of the coincidence electronics. As previously described by Bodi et al.,[36] any single-start/single-stop coincidence measurement necessarily suppresses the populations of all species recorded in a TOF spectrum. The degree of this suppression increases with the total count rate and, importantly, the TOF of the species, so that the heavier parent ion signals are reduced relative to the lighter daughter ion signals. Because a large amount of thermochemical data has been acquired by using the single-start/single-stop TPEPICO method without accounting for this bias under the assumption that its effect is far smaller than the uncertainty in the measurement, it is worth experimentally evaluating the validity of this assumption. Comparison of TPEPICO spectra of vinyl iodide obtained under both moderate and low paralysis conditions allows for the determination of the actual magnitude of the effect, the comparison to the predicted magnitude, and the evaluation of the efficacy of a scheme to correct spectra for the paralysis effects.

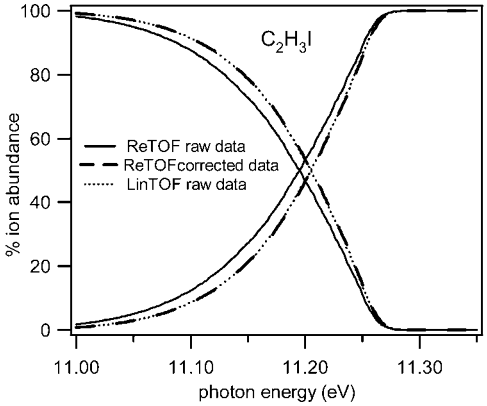

Figure A2. Best-fit breakdown curves of $C_2H_3I \rightarrow C_2H_3^+ + I$ to experimental data obtained on the LinTOF (the same data as in Figure 4) and the ReTOF and paralysis-corrected ReTOF data. Note that the LinTOf and corrected ReTOF data are nearly identical.

Figure A1 shows two spectra obtained with the ReTOF MS at the same photon energy but with different sample pressures and light source intensities in order to produce significantly different ion count rates. The relative fragment (50 μs TOF) and parent (135 μs TOF) ion intensities differ between the high and low ion count rate spectra; because the photon energies are identical, this must be an experimental artifact. In high count rate experiments, electron and ion signals from one photoionization event become interleaved with another electron and ion signal pair. As a result, a start signal from one ionization event may be stopped by an ion from a previous ionization event (a false coincidence), thereby suppressing the true ion. This has the effect of suppressing the heavier ion, which arrives at a later TOF.

The sloping background apparent in the 8000 ion c/s spectrum but absent in the 1000 c/s spectrum, in Figure A1 is a clear marker of signal paralysis. In the limit where false coincidences greatly outnumber true coincidences, the factor by which counts at any TOF are suppressed is equal to the ratio of the baseline height at that TOF and the baseline height at time zero. From Figure 1, the parent ion (baseline counts ≈ 80) in the 8000 c/s spectrum is suppressed by a factor of about 2.2 more than the daughter ion (baseline counts ≈ 175), whereas in the 1000 c/s spectrum (with a level baseline), the suppression of the two peaks is nearly identical. The relative peak areas of the high count spectrum could be corrected by that factor of 2.2, whereas the low count spectrum would require no paralysis correction at all.

Although easily assessable by inspection, comparison of baseline heights gives only an approximate correction factor to the true coincidence peaks areas. False coincidences are paralyzed by both earlier arriving false and true coincidences, whereas true coincidences are paralyzed only by false coincidences (because there is only one true coincidence for every start signal, there cannot be any earlier arriving true coincidences). As a result, false coincidences (which make up the baseline) suffer a different degree of paralysis than true coincidences arriving at the same TOF. In the data analysis used here, we employed a less intuitive but more rigorous correction scheme based on the formalism described by Bodi et al.[36]

However, for the moderate extent of the paralysis in these data, the results are essentially identical.

The vinyl iodide data were collected with the LinTOF and the ReTOF. Because the former has a TOF that is approximately five times less than that of the ReTOF data, the paralysis is correspondingly less to the extent that its effects are negligible. Best-fit breakdown curves of the vinyl iodide data are shown in Figure A2. The raw ReTOF curve differs significantly from the LinTOF data; however, the paralysis-corrected ReTOF curve is identical to the LinTOF data. This suggests that paralysis effects are inline with those predicted by Bodi et al. and easily corrected for.

It is interesting that the paralysis affects the breakdown diagram most strongly near the cross-over region and very little near the 0 K dissociation limit of 11.262 eV. This indicates that the extraction of the 0 K dissociation onset is not affected significantly by the paralysis. On the other hand, the assumed temperature for fitting the paralysis-uncorrected data would be higher than the temperature needed to fit the corrected data.

Acknowledgment. We thank the U.S. Department of Energy, Office of Basic Energy Sciences, for financial support. M.A.O. thanks Project SEED, funded by the American Chemical Society, the Burroughs-Wellcome Fund, and the Hamner Institute for Life Sciences for a summer high-school student fellowship.

References and Notes

(1) Kolesov, V. P.; Papina, T. S. *Russ. J. Phys. Chem.* **1970**, *44* (4), 611–613.

(2) Lacher, J. R.; Kianpour, A.; Montgomery, P.; Knedler, H.; Park, J. D. *J. Phys. Chem.* **1957**, *61* (8), 1125–1126.

(3) Lago, A. F.; Baer, T. *J. Phys. Chem. A* **2006**, *110* (9), 3036–3041.

(4) Levanova, S. V.; Treger, Y. A.; Velichko, S. M.; Rozhnov, A. M.; Khlestkov, A. I.; Pisarev, V. V. *J. Appl. Chem. USSR* **1975**, *48* (7), 1628–1631.

(5) Joshi, R. M. *Indian J. Chem.* **1964**, *2* (3), 125.

(6) Sheng, L. S.; Qi, F.; Tao, L.; Zhang, Y. W.; Yu, S. Q.; Wong, C. K.; Li, W. K. *Int. J. Mass Spectrom. Ion Processes* **1995**, *148* (3), 179–189.

(7) Lacher, J. R.; Park, J. D.; Gottlieb, H. B. *Trans. Faraday Soc.* **1962**, *58* (DEC), 2348.

(8) Lacher, J. R.; Emery, E.; Bohmfalk, E.; Park, J. D. *J. Phys. Chem.* **1956**, *60* (4), 492–495.

(9) Manion, J. A. *J. Phys. Chem. Ref. Data* **2002**, *31* (1), 123–172.

(10) Colegrove, B. T.; Thompson, T. B. *J. Chem. Phys.* **1997**, *106* (4), 1480–1490.

(11) Luo, Y. R.; Holmes, J. L. *J. Phys. Chem.* **1992**, *96* (23), 9568–9571.

(12) Alfassi, Z. B.; Golden, D. M.; Benson, S. W. *J. Chem. Thermodyn.* **1973**, *5* (3), 411–420.

(13) Harding, M. E.; Gauss, J.; Pfluger, K.; Werner, H.-J. *J. Phys. Chem. A* **2007**, *111* (51), 13623–13628.

(14) The anharmonic corrections to the 298 K heats of formation reported by Harding et al. were in error. Harding has provided us with the correct 298 K value for vinyl chloride for use here and an erratum is in press (JPCA).

(15) Pedley, J. B. *Thermochemical Data and Structures of Organic Compounds*; Thermodynamics Research Center: College Station, TX, 1994; Vol. I.

(16) Luo, Y.-R. *Comprehensive Handbook of Chemical Bond Energies*; CRC Press: Boca Raton, FL, 2007.

(17) Gurvich, L. V.; Veyts, I. V.; Alcock, C. B. *Thermodynamic Propeties of Individual Substances*; 4 ed.; Hemisphere: New York, 1991.

(18) Cao, J. R.; Zhang, J. M.; Zhong, X.; Huang, Y. H.; Fang, W. Q.; Wu, X. J.; Zhu, Q. H. *Chem. Phys.* **1989**, *138* (2−3), 377–382.

(19) Glukhovtsev, M. N.; Bach, R. D. *J. Phys. Chem. A* **1997**, *101* (19), 3574–3579.

(20) Sztaray, B.; Baer, T. *Rev. Sci. Instrum.* **2003**, *74* (8), 3763–3768.

(21) Baer, T.; Sztaray, B.; Kercher, J. P.; Lago, A. F.; Bodi, A.; Skull, C.; Palathinkal, D. *Phys. Chem. Chem. Phys.* **2005**, *7* (7), 1507–1513.

(22) Zhang, P.; Li, J.; Mo, Y. X. *J. Phys.Chem. A* **2007**, *111* (35), 8531–8535.

(23) Chang, J. L.; Shieh, J. C.; Wu, J. C.; Li, R. H.; Chen, Y. T. *Chem. Phys. Lett.* **2000**, *325* (4), 369–374.

(24) Locht, R.; Leyh, B.; Hottmann, K.; Baumgartel, H. *Chem. Phys.* **1997**, *220* (1−2), 217–232.

(25) Lee, M.; Kim, M. S. *J. Phys. Chem. A* **2007**, *111* (34), 8409–8415.

(26) Sze, K. H.; Brion, C. E.; Katrib, A.; Elissa, B. *Chem. Phys.* **1989**, *137* (1−3), 369–390.

(27) Kishimoto, N.; Ohshimo, K.; Ohno, K. *J. Electron Spectrosc. Relat. Phenom.* **1999**, *104* (1−3), 145–154.

(28) Boschi, R. A. A.; Salahub, D. R. *Can. J. Chem.* **1974**, *52* (8), 1217–1228.

(29) Mines, G. W.; Thompson, H. W. *Spectrochim. Acta, Part A* **1973**, *A 29* (7), 1377–1383.

(30) Chase, M. W. *NIST-JANAF Thermochemical Tables*; 4th ed.; American Institute of Physics: Woodbury, New York, 1998.

(31) Ritter, E. R. *J. Chem. Inf. Comput. Sci.* **1991**, *31* (3), 400–408.

(32) Frisch, M. J.; Trucks, G. W.; Schlegel, H. B.; Scuseria, G. E.; Robb, M. A.; Cheeseman, J. R.; Montgomery, J. A., Jr.; Vreven, T.; Kudin, K. N.; Burant, J. C.; Millam, J. M.; Iyengar, S. S.; Tomasi, J.; Barone, V.; Mennucci, B.; Cossi, M.; Scalmani, G.; Rega, N.; Petersson, G. A.; Nakatsuji, H.; Hada, M.; Ehara, M.; Toyota, K.; Fukuda, R.; Hasegawa, J.; Ishida, M.; Nakajima, T.; Honda, Y.; Kitao, O.; Nakai, H.; Klene, M.; Li, X.; Knox, J. E.; Hratchian, H. P.; Cross, J. B.; Bakken, V.; Adamo, C.; Jaramillo, J.; Gomperts, R.; Stratmann, R. E.; Yazyev, O.; Austin, A. J.; Cammi, R.; Pomelli, C.; Ochterski, J. W.; Ayala, P. Y.; Morokuma, K.; Voth, G. A.; Salvador, P.; Dannenberg, J. J.; Zakrzewski, V. G.; Dapprich, S.; Daniels, A. D.; Strain, M. C.; Farkas, O.; Malick, D. K.; Rabuck, A. D.; Raghavachari, K.; Foresman, J. B.; Ortiz, J. V.; Cui, Q.; Baboul, A. G.; Clifford, S.; Cioslowski, J.; Stefanov, B. B.; Liu, G.; Liashenko, A.; Piskorz, P.; Komaromi, I.; Martin, R. L.; Fox, D. J.; Keith, T.; Al-Laham, M. A.; Peng, C. Y.; Nanayakkara, A.; Challacombe, M.; Gill, P. M. W.; Johnson, B.; Chen, W.; Wong, M. W.; Gonzalez, C.; Pople, J. A. *Gaussian 03*, revision C.02; Gaussian, Inc.: Wallingford, CT, 2007.

(33) Ruscic, B.; Boggs, J. E.; Burcat, A.; Csaszar, A. G.; Demaison, J.; Janoschek, R.; Martin, J. M. L.; Morton, M. L.; Rossi, M. J.; Stanton, J. F.; Szalay, P. G.; Westmoreland, P. R.; Zabel, F.; Berces, T. *J. Phys. Chem. Ref. Data* **2005**, *34* (2), 573–656.

(34) Schuchardt, K. L.; Didier, B. T.; Elsethagen, T.; Sun, L. S.; Gurumoorthi, V.; Chase, J.; Li, J.; Windus, T. L. *J. Chem. Inf. Model.* **2007**, *47* (3), 1045–1052.

(35) Ruscic, B.; Pinzon, R. E.; Morton, M. L.; von Laszevski, G.; Bittner, S. J.; Nijsure, S. G.; Amin, K. A.; Minkoff, M.; Wagner, A. F. *J. Phys. Chem. A* **2004**, *108* (45), 9979–9997.

(36) Bodi, A.; Sztaray, B.; Baer, T.; Johnson, M.; Gerber, T. *Rev. Sci. Instrum.* **2007**, *78* (8), 084102.

JP8007255